

Efficient Entanglement Swapping in High-Dimensions with only Linear Optics

Baghdasar Bagdasaryan,^{1,*} Kaushik Joarder,¹ and Fabian Steinlechner^{1, 2, 3, †}

¹*Institute of Applied Physics, Friedrich Schiller University Jena, 07745 Jena, Germany.*

²*Abbe Center of Photonics, Friedrich Schiller University Jena, 07745 Jena, Germany.*

³*Fraunhofer Institute for Applied Optics and Precision Engineering, 07745 Jena, Germany*

(Dated: October 20, 2025)

Entanglement swapping is a fundamental building block for realizing first-generation quantum repeaters, which are essential for building global quantum networks. Current quantum repeater systems still struggle to achieve practical communication rates. High-dimensional (HD) encoding can significantly improve repeater efficiency by boosting information capacity and enhancing noise tolerance and security. However, the experimental demonstration of this protocol so far has been limited only to two-dimensional systems due to the requirement of strong nonlinear interactions. Here, we introduce an efficient linear-optics protocol for HD entanglement swapping that uses ancillary photons and is compatible with arbitrary photonic degrees of freedom (DOFs). We further show that photon-number-resolving detectors substantially enhance the performance of the setup and become especially valuable for dimensions beyond six. For a four-dimensional scenario, we present an experimental design using hyper-entanglement in polarization and time-bin DOFs. This setup resolves the most challenging part of the ancillary photons-based approach, namely the necessary preparation of the ancilla state and analysis of the resulting swapped state.

I. INTRODUCTION

Realizing large-scale quantum communication networks [1–6] hinges on key protocols such as quantum teleportation [7] and entanglement swapping [8]. The teleportation uses entanglement to transfer unknown states at a distance, while entanglement swapping relays entanglement across network nodes.

Since the first demonstration of quantum teleportation [9] and entanglement swapping [10], significant progress has been made to enhance these protocols [11–17], including the generalization to multiple particles, a necessary step for scaling quantum networks [18–20]. Most of these protocols have been realized using polarization- or path-entangled qubits, i.e., two-level quantum systems. However, it is well established that high-dimensional (HD) quantum states, qudits, offer several advantages over their two-dimensional counterparts. These include higher information capacity, greater robustness against eavesdropping and quantum cloning, stronger violations of local realism, and enhanced potential for quantum computation [21–23].

Photonic quantum technologies have made great progress, both as a scalable quantum information platform [24, 25] as well as the network-enabling ability to interconnect different processing nodes [26]. A key challenge in implementing HD variants of entanglement swapping [27, 28] or quantum teleportation lies in two main areas: the preparation and verification of HD entangled states [29–32], and the realization of the Bell state measurement (BSM) [33]. This latter difficulty arises because linear optics BSM typically relies on Hong-Ou-Mandel (HOM) interference on a two-port beam splitter.

Extending this approach to higher dimensions often necessitates the use of ancilla photons or nonlinear media [34]. The first attempts were to teleport two-qubit composite systems [35], teleport multiple degrees of freedom (DOFs) of a single photon [36], perform simultaneous entanglement swapping of different qubit systems in orbital angular momentum DOF [37] or frequency DOF [38].

Initial HD teleportation protocols were implemented in path DOF using ancilla photons to perform the HD BSM [39, 40]. Subsequent studies demonstrated that a BSM can be achieved through hyper-entanglement [41], by using the Greenberger-Horne-Zeilinger state [42], by exploiting multiple squeezer devices [43] utilizing sum frequency generation [44, 45], by using Quantum autoencoders to reconstruct qudit states [46] or by using linear optics and permutation-entangled states as resource [47]. Recent work [48] discussed the utilization of quantum Fourier transform (QFT) with linear optics for implementing the HD BSM, tailored to time-bin encoding in even dimensions. Implementation of D -dimensional QFT scales quadratically in number of required beam splitters [49]. The large number of beam splitters will cause an exponential decrease in the fidelity of the final state if perfect HOM interference is not ensured.

Despite significant progress, the experimental demonstration of HD entanglement swapping remains elusive. This is partly due to the lack of BSM approaches that can be tailored to the specific challenges of time-bin, spatial mode, or frequency encoding. To address this, we introduce a setup for designing BSM up to six dimensions using linear optical quantum computing and ancillary photons. Moreover, the scheme is applicable across any DOFs and technological platforms. To showcase this, we further discuss a concrete experimental setup for realizing entanglement swapping with hyper-entangled states in time-bin [50–53] and polarization DOFs [54–56].

This manuscript is organized into three main Sections.

* baghdasar.bagdasaryan@uni-jena.de

† fabian.steinlechner@uni-jena.de

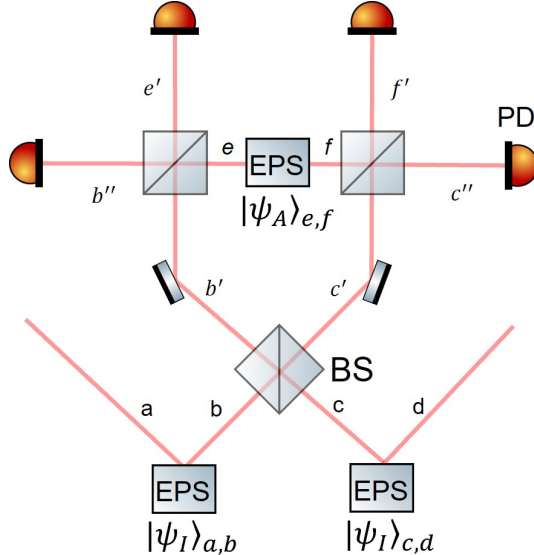


FIG. 1: Schematic of three- and four-dimensional entanglement swapping with three 50:50 beam splitters (**BS**). In addition to two initially maximally entangled states, the setup also contains a two-dimensional ancilla state for performing the BSM. **EPS**: entangled photon-pair source; **PD**: photon detector.

Section II outlines the general implementation of four- and six-dimensional BSM. Following this, Section III proposes a specific implementation of four-dimensional BSM, leveraging hyper-entanglement across time-bin and polarization DOFs. Finally, Section IV provides the conclusion.

II. SCHEME AND ANALYSIS FOR HD ENTANGLEMENT SWAPPING

A. Four-dimensional entanglement swapping

The schematic for four-dimensional entanglement swapping is shown in Fig. 1. The initial states can be any of 16 orthogonal entangled Bell-like states in four dimensions [57]. The derivation is shown only for

$$|\psi_I\rangle_{m,n} = \frac{1}{2} \left(|1,1\rangle_{m,n} + |2,2\rangle_{m,n} + |3,3\rangle_{m,n} + |4,4\rangle_{m,n} \right), \quad (1)$$

as it is analogous to all other four-dimensional Bell states. Here, I refers to the initial state, the subscripts m and n denote the spatial modes, and the internal mode numbers 1 – 4 correspond to the orthogonal states in any DOF in

which the entanglement is encoded. The initial state consists of the first entangled state in spatial modes a and b , denoted as $|\psi_I\rangle_{a,b}$ and the second entangled state in spatial modes c and d , $|\psi_I\rangle_{c,d}$. A complete HD BSM cannot be implemented with linear optics only [58]. Therefore, in addition to the initial states, we consider a maximally entangled ancillary state, which is prepared in spatial modes e and f , $|\psi_A\rangle_{e,f}$. Therefore, the composite state of all three subsystems reads as $|\psi_I\rangle_{a,b} |\psi_I\rangle_{c,d} |\psi_A\rangle_{e,f}$.

In the first step, we apply a 50 : 50 beam splitter operation on photons in paths b and c . For instance, the beam splitter transformation of the term $|1,1\rangle_{a,b} |1,1\rangle_{c,d}$ yields

$$|1,1\rangle_{a,b} |1,1\rangle_{c,d} \rightarrow \frac{1}{2} |1\rangle_a |1\rangle_d \left(|1\rangle_{b'} |1\rangle_{c'} - |1\rangle_{b'} |1\rangle_{c'} \right. \\ \left. + i |1\rangle_{b'} |1\rangle_{b'} |vac\rangle_{c'} + i |vac\rangle_{b'} |1\rangle_{c'} |1\rangle_{c'} \right). \quad (2)$$

The first two terms in brackets cancel each other out if the indistinguishability of photons is ensured. Therefore, the transformation (2) contains no terms where photons exit in different spatial modes. In contrast, the transformation of $|1,1\rangle_{a,b} |2,2\rangle_{c,d}$ results in

$$|1,1\rangle_{a,b} |2,2\rangle_{c,d} \rightarrow \frac{1}{2} |1\rangle_a |2\rangle_d \left(|1\rangle_{b'} |2\rangle_{c'} - |2\rangle_{b'} |1\rangle_{c'} \right. \\ \left. + i |1\rangle_{b'} |2\rangle_{b'} |vac\rangle_{c'} + i |vac\rangle_{b'} |1\rangle_{c'} |2\rangle_{c'} \right).$$

The notation $|2\rangle_{c'}$ means a single photon in the spatial mode c' with internal DOF of 2 and should not be confused with Fock state notation.

As we will post-select only those events where all four detectors click, we focus only on the terms where the photons exit the beam splitter through different spatial modes. Therefore, from the transformation of $|1,1\rangle_{a,b} |2,2\rangle_{c,d}$, we only retain the following term:

$$|1\rangle_a |2\rangle_d \left(|1\rangle_{b'} |2\rangle_{c'} - |2\rangle_{b'} |1\rangle_{c'} \right) = |1\rangle_a |2\rangle_d |\psi_{1,2}^-\rangle_{b',c'}.$$

Here, we have used the notation for the Bell state:

$$|\psi_{k,j}^-\rangle_{m,n} = \frac{1}{\sqrt{2}} \left(|k,j\rangle_{m,n} - |j,k\rangle_{m,n} \right).$$

Similarly, the transformation of $|2,2\rangle_{a,b} |1,1\rangle_{c,d}$ yields the term $-|2\rangle_a |1\rangle_d |\psi_{1,2}^-\rangle_{b',c'}$. Combining these relevant modes ultimately results in $|\psi_{1,2}^-\rangle_{a,d} |\psi_{1,2}^-\rangle_{b',c'}$. Applying the same derivation steps for other mode combinations, the transformation of the two initial states $|\psi_I\rangle_{a,b} |\psi_I\rangle_{c,d}$ after the first beam splitter can be expressed in an unnormalized form as:

$$|\psi_{1,2}^-\rangle_{a,d} |\psi_{1,2}^-\rangle_{b',c'} + |\psi_{1,3}^-\rangle_{a,d} |\psi_{1,3}^-\rangle_{b',c'} + |\psi_{1,4}^-\rangle_{a,d} |\psi_{1,4}^-\rangle_{b',c'} + |\psi_{2,3}^-\rangle_{a,d} |\psi_{2,3}^-\rangle_{b',c'} + |\psi_{2,4}^-\rangle_{a,d} |\psi_{2,4}^-\rangle_{b',c'} + |\psi_{3,4}^-\rangle_{a,d} |\psi_{3,4}^-\rangle_{b',c'} . \quad (3)$$

After the first beam splitter, the state of four photons is a coherent superposition of products of two-dimensional Bell states. To engineer a genuine four-dimensional entangled state in modes a and d , we must coherently combine specific pairs of these singlets. For example, we might aim to combine the terms $|\psi_{1,2}^-\rangle_{a,d}$ and $|\psi_{3,4}^-\rangle_{a,d}$, which appear in the first and last terms of Eq. (3), to have the four-dimensional maximally entangled state $1/\sqrt{2}(|\psi_{1,2}^-\rangle_{a,d} + |\psi_{3,4}^-\rangle_{a,d})$. To achieve this coherent combination, the relevant terms must share a common product component, allowing us to factor out the desired superposition, such as $(|\psi_{1,2}^-\rangle_{a,d} + |\psi_{3,4}^-\rangle_{a,d}) \times (\text{common product})$. Given that the first term is accompanied by $|\psi_{1,2}^-\rangle_{b',c'}$ and the second with $|\psi_{3,4}^-\rangle_{b',c'}$, the $|\psi_{1,2}^-\rangle_{b',c'}$ component needs to interfere with ancillary mode $|3,4\rangle_{e,f}$, while the term $|\psi_{3,4}^-\rangle_{b',c'}$ with ancillary mode $|1,2\rangle_{e,f}$. This interference can be accomplished by preparing the ancillary state in a superposition of these modes:

$$|\psi_A\rangle_{e,f} = \frac{1}{\sqrt{2}}(|1,2\rangle_{e,f} + |3,4\rangle_{e,f}). \quad (4)$$

We analyze the interference of the remaining state (3) with the ancilla state (4) as shown in Fig. 1. The two beam splitter transformations applied to each term in (3) yield:

$$\begin{aligned} |\psi_{1,2}^-\rangle_{a,d} |\psi_{1,2}^-\rangle_{b',c'} |\psi_A\rangle_{e,f} &\rightarrow \frac{1}{4} |\psi_{1,2}^-\rangle_{a,d} \left(-|\psi_{2,1}^-\rangle_{b'',e'} |\psi_{1,2}^-\rangle_{c'',f'} + |\psi_{1,3}^-\rangle_{b'',e'} |\psi_{2,4}^-\rangle_{c'',f'} - |\psi_{2,3}^-\rangle_{b'',e'} |\psi_{1,4}^-\rangle_{c'',f'} \right), \\ |\psi_{1,3}^-\rangle_{a,d} |\psi_{1,3}^-\rangle_{b',c'} |\psi_A\rangle_{e,f} &\rightarrow \frac{1}{4} |\psi_{1,3}^-\rangle_{a,d} \left(|\psi_{1,3}^-\rangle_{b'',e'} |\psi_{3,4}^-\rangle_{c'',f'} - |\psi_{3,1}^-\rangle_{b'',e'} |\psi_{1,2}^-\rangle_{c'',f'} \right), \\ |\psi_{1,4}^-\rangle_{a,d} |\psi_{1,4}^-\rangle_{b',c'} |\psi_A\rangle_{e,f} &\rightarrow \frac{1}{4} |\psi_{1,4}^-\rangle_{a,d} \left(-|\psi_{4,1}^-\rangle_{b'',e'} |\psi_{1,2}^-\rangle_{c'',f'} - |\psi_{4,3}^-\rangle_{b'',e'} |\psi_{1,4}^-\rangle_{c'',f'} \right), \\ |\psi_{2,3}^-\rangle_{a,d} |\psi_{2,3}^-\rangle_{b',c'} |\psi_A\rangle_{e,f} &\rightarrow \frac{1}{4} |\psi_{2,3}^-\rangle_{a,d} \left(|\psi_{2,1}^-\rangle_{b'',e'} |\psi_{3,2}^-\rangle_{c'',f'} + |\psi_{2,3}^-\rangle_{b'',e'} |\psi_{3,4}^-\rangle_{c'',f'} \right), \\ |\psi_{2,4}^-\rangle_{a,d} |\psi_{2,4}^-\rangle_{b',c'} |\psi_A\rangle_{e,f} &\rightarrow \frac{1}{4} |\psi_{2,4}^-\rangle_{a,d} \left(|\psi_{2,1}^-\rangle_{b'',e'} |\psi_{4,2}^-\rangle_{c'',f'} - |\psi_{4,3}^-\rangle_{b'',e'} |\psi_{2,4}^-\rangle_{c'',f'} \right), \\ |\psi_{3,4}^-\rangle_{a,d} |\psi_{3,4}^-\rangle_{b',c'} |\psi_A\rangle_{e,f} &\rightarrow \frac{1}{4} |\psi_{3,4}^-\rangle_{a,d} \left(|\psi_{1,3}^-\rangle_{b'',e'} |\psi_{2,4}^-\rangle_{c'',f'} - |\psi_{4,1}^-\rangle_{b'',e'} |\psi_{3,2}^-\rangle_{c'',f'} - |\psi_{4,3}^-\rangle_{b'',e'} |\psi_{3,4}^-\rangle_{c'',f'} \right). \end{aligned}$$

Among all possible Bell state combinations, only the term $|\psi_{1,3}^-\rangle_{b'',e'} |\psi_{2,4}^-\rangle_{c'',f'}$ appears twice in the brackets. This is a direct consequence of our ancillary state choice. For example, selecting the state $\frac{1}{\sqrt{2}}(|1,4\rangle_{e,f} + |2,3\rangle_{e,f})$ would instead lead to the term $|\psi_{1,2}^-\rangle_{b'',e'} |\psi_{4,3}^-\rangle_{c'',f'}$ appearing twice. Through post-selection of this specific term, the unnormalized composite state is then:

$$\left(|\psi_{1,2}^-\rangle_{a,d} + |\psi_{3,4}^-\rangle_{a,d} \right) |\psi_{1,3}^-\rangle_{b'',e'} |\psi_{2,4}^-\rangle_{c'',f'}.$$

Therefore, when photons in spatial modes b'' and e' are projected onto the Bell state $|\psi_{1,3}^-\rangle_{b'',e'}$ and photons in spatial modes c'' and f' are projected onto $|\psi_{2,4}^-\rangle_{c'',f'}$, the state of remaining photons in spatial modes a and d becomes the four-dimensional maximally entangled state:

$$\frac{1}{2}(|1,2\rangle_{a,d} - |2,1\rangle_{a,d} + |3,4\rangle_{a,d} - |4,3\rangle_{a,d}).$$

The projection into these Bell states is achieved by measuring four-photon coincidences with four possible mode combinations $\{3,1,4,2\}$, $\{3,1,2,4\}$, $\{1,3,4,2\}$ and $\{1,3,2,4\}$ in detectors at outputs $\{b'',e',f',c''\}$. Any other four-photon coincidence event projects the state of photons in modes a and d into a two-dimensional

Bell state. Note that the relative phase between modes $(|1,2\rangle_{a,d} - |2,1\rangle_{a,d})$ and $(|3,4\rangle_{a,d} - |4,3\rangle_{a,d})$ can be controlled by adjusting the phase between the two modes of the ancilla state.

The interferometric part of the scheme in Fig. 1 can be implemented on a programmable photonic quantum processor. With flexible output-mode assignment, one can also herald four-dimensional states on spatial modes other than a and d . In the second line of the multiline expression following Eq. (4), the state factorizes as

$$|\psi_{1,3}^-\rangle_{a,d} |\psi_{1,3}^-\rangle_{b'',e'} \left(|\psi_{1,2}^-\rangle_{c'',f'} + |\psi_{3,4}^-\rangle_{c'',f'} \right), \quad (5)$$

and in the fifth line as

$$|\psi_{2,4}^-\rangle_{a,d} |\psi_{4,2}^-\rangle_{c'',f'} \left(|\psi_{2,1}^-\rangle_{b'',e'} + |\psi_{4,3}^-\rangle_{b'',e'} \right). \quad (6)$$

Consequently, for example, projecting the photons in modes a and d into the Bell state $|\psi_{1,3}^-\rangle_{a,d}$ and the photons in b'' and e' into $|\psi_{1,3}^-\rangle_{b'',e'}$ heralds the four dimensional state in modes c'' and f' :

$$\frac{1}{2}(|1,2\rangle_{c'',f'} - |2,1\rangle_{c'',f'} + |3,4\rangle_{c'',f'} - |4,3\rangle_{c'',f'}).$$

This flexibility yields eight additional detection patterns that herald a four-dimensional entangled state. The same

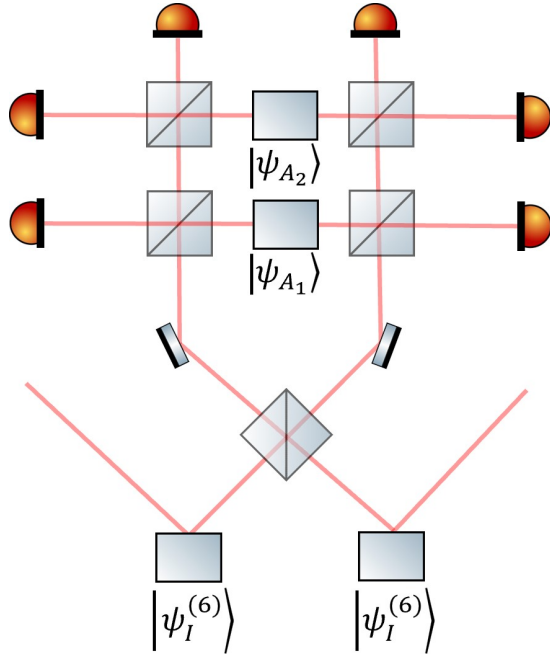


FIG. 2: Schematic of five- and six-dimensional entanglement swapping with two two-dimensional ancilla Bell states.

architecture in Fig. 1 can also realize three-dimensional entanglement swapping, which reduces the number of occupied modes and thereby increases the overall success probability (see Appendix).

B. Five- and six-dimensional entanglement swapping

The scheme in Fig. 1 can be extended to higher dimensions. For instance, Fig. 2 illustrates the setup for five- or six-dimensional entanglement swapping, which now requires two entangled ancilla states. The initial states for the six-dimensional scenario are again the generalized Bell states, for instance:

$$|\psi_I^{(6)}\rangle_{m,n} = \frac{1}{\sqrt{6}}(|1,1\rangle_{m,n} + |2,2\rangle_{m,n} + |3,3\rangle_{m,n} + |4,4\rangle_{m,n} + |5,5\rangle_{m,n} + |6,6\rangle_{m,n}).$$

The ancilla states are again two dimensional maximally entangled states $|\psi_{A_1}\rangle_{m,n} = 1/\sqrt{2}(|1,2\rangle_{m,n} + |3,4\rangle_{m,n})$ and $|\psi_{A_2}\rangle_{m,n} = 1/\sqrt{2}(|5,6\rangle_{m,n} + |3,4\rangle_{m,n})$. In order to achieve six-dimensional entanglement swapping, all interfered photons need to be detected in distinct modes as in the previous example, i.e., $\{1,2,3,4,5,6\}$. As expected, the scheme in Fig. 2 is less efficient compared to the four-dimensional case. The total number of possible detection events is 106,632, out of which only four lead to the desired entangled state, making its implementation in the near future very challenging. The success probability can

be increased with photon-number-resolving (PNR) capabilities, where photons arriving in the same spatial mode can be detected with high efficiency. Discussion of the generalized scheme for higher D -dimensions is omitted here, as its implementation would result in even lower efficiency.

C. Success probability

To estimate the total efficiency of the four-dimensional entanglement swapping, the normalization factor of the final heralded state can be calculated. Each of the two initial entangled four-dimensional states carries a factor of $1/2$. The scheme uses one ancillary Bell pair normalized by $1/\sqrt{2}$. The number of beam splitter operations is 3, where each operation acts on two photons and introduces a factor of $1/2$. The overall normalization factor reads as

$$\left(\frac{1}{\sqrt{2}2^4}\right)\frac{1}{2}(|1,2\rangle_{a,d} - |2,1\rangle_{a,d} + |3,4\rangle_{a,d} - |4,3\rangle_{a,d}).$$

The last term $1/2$ is retained as the normalization factor of the heralded four-dimensional state. The probability of a single, specific heralded event is the square of the amplitude within the brackets, $1/2^9$. As four possible measurement outcomes successfully herald a four-dimensional entangled state in modes a and d , the total success probability is $4/2^9$. If different output modes other than a and d are permitted, then the success probability becomes $12/2^9$ following from Eqs. (5) and (6).

Inherently, a significant fraction of photons is lost since the scheme relies on ancilla photons and only considers bunched photon events. Nevertheless, an attractive aspect of this scheme is that the remaining four-photon events still herald useful two-dimensional Bell states. For instance, the detection event with mode numbers $\{2,1,1,2\}$ leads to the Bell state $|\psi_{1,2}^-\rangle_{a,d}$, which follows from the first term in the multiline expression after Eq. (4). There are in total 48 four-photon events leading to two-dimensional swapping with success probability $48/2^{10}$. This feature could be useful in scenarios where both two-dimensional and four-dimensional states are required for different protocols.

Employing PNR detectors significantly enhances the success probability, as they can distinguish multiple photons occupying the same internal mode and sharing the same spatial mode. With PNR detection, the number of events leading to four-dimensional entanglement swapping is 16 and to two-dimensional entanglement swapping is 552, corresponding to success probabilities of $16/2^9$ for four-dimensional and $552/2^{10} \approx 0.54$ for two-dimensional entanglement swapping. If the output modes can be chosen flexibly, the success probability of heralding a two-dimensional entangled state increases to $828/2^{10} \approx 0.8$. The terms corresponding to these events are not presented in the multiline expression after Eq. (4), since we

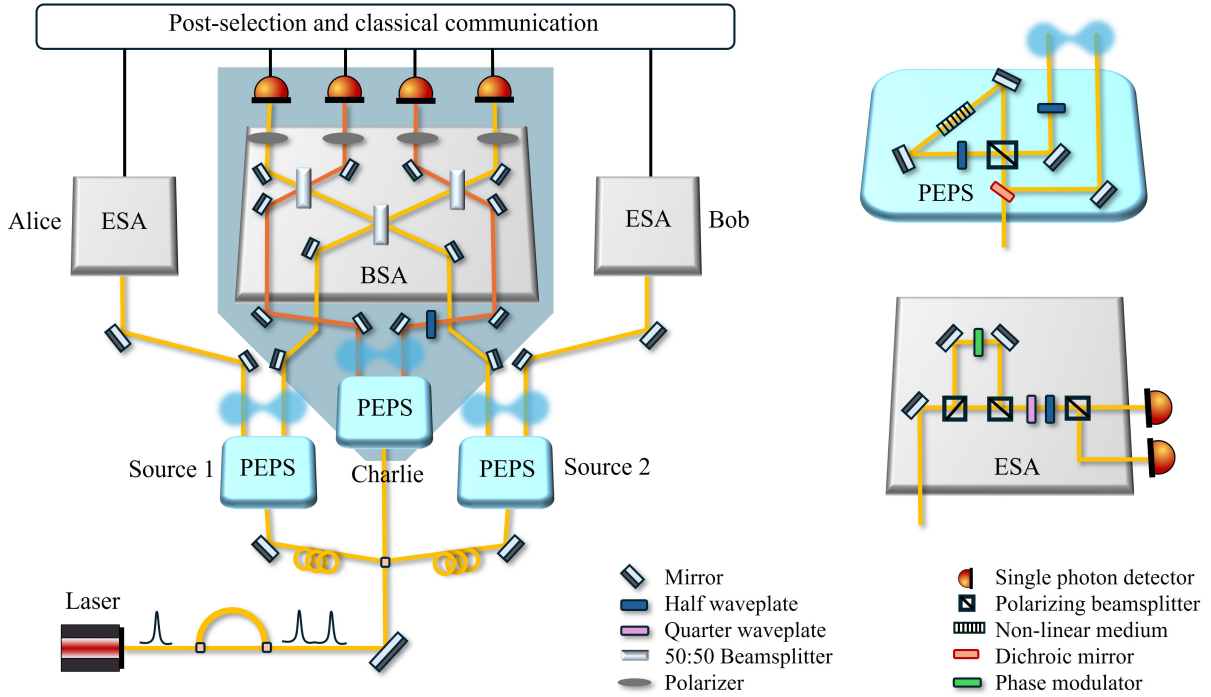


FIG. 3: Proposed experimental setup for four-dimensional entanglement swapping using hyper-entanglement in time-bin and polarization DOFs. **PEPS**: polarization-entangled photon-pair source; **BSA**: Bell state analyzer; **ESA**: entangled state analyzer.

only considered the terms that correspond to bunched photon events (different spatial modes for all photons).

With two-dimensional input states, passive elements, no ancilla or feed-forward, and threshold detection, a BSM can unambiguously distinguish at most two of the four Bell states, bounding the success probability at $\leq 50\%$. Notably, the probability for two-dimensional swapping surpasses the conventional 50% limit. This improvement becomes possible because our scheme already incorporates HD states and ancillary photons, as discussed in [15, 59, 60]. Our approach, therefore, not only enables HD entanglement swapping but also surpasses the conventional 50% success probability limit for setups based solely on passive, linear optical elements.

In addition to the success probability, the fidelity of the final state is also a critical performance metric. All schemes based on the HOM effect suffer from fidelity degradation at each stage of beam splitter operation. We can define a HOM interference efficiency η , which depends on the HOM visibility. For a sequence of N beam splitters, the fidelity decreases as η^N , resulting in an exponential decay. Since achieving 100% visibility is extremely challenging, this exponential degradation is unavoidable in practice. Consequently, there is an inherent trade-off between achieving a high success probability in HD BSM and maintaining the fidelity of the final state. We conclude that, with current technology, entanglement swapping in very high dimensions is not practically feasible. For low-dimensional setups, however, incorporating

PNR capabilities is essential to achieving both high success probability and acceptable fidelity.

III. PROPOSAL: EXPERIMENTAL SETUP FOR FOUR-DIMENSIONAL ENTANGLEMENT SWAPPING

We consider a four-dimensional entangled state encoded in a hyper-entangled form, using both time-bin and polarization DOFs. The use of hyper-entanglement makes the preparation of ancillary states and the verification of the final swapped state experimentally practical. Moreover, the use of hyper-entangled states enables the manipulation and measurement of each DOF independently with well-established linear optical techniques.

A four-dimensional hyper-entangled state in both sources 1 and 2 (Fig. 3) is prepared by using a polarization-entangled pair source (PEPS) pumped with two mutually coherent pulses: early and late pulses. The output photon pair becomes the hyper-entangled state:

$$|\psi_I\rangle_{m,n} = \frac{1}{2} \left(|H(t_e), H(t_e)\rangle_{m,n} + |V(t_e), V(t_e)\rangle_{m,n} \right. \\ \left. + |H(t_l), H(t_l)\rangle_{m,n} + |V(t_l), V(t_l)\rangle_{m,n} \right). \quad (7)$$

Here $t_{e(l)}$ represents the early (late) time-bin state of the photon, and $|H(V)\rangle$ shows the horizontal (vertical) polarization state. The state in Eq. (7) is equivalent to the

four-dimensional entangled state in Eq. (1), once we assign the values $|1\rangle = |H(t_e)\rangle$, $|2\rangle = |V(t_e)\rangle$, $|3\rangle = |H(t_l)\rangle$, $|4\rangle = |V(t_l)\rangle$.

To ensure optimal time synchronization and photon indistinguishability within the Bell state analyzer (BSA), a single master laser pumps the PEPSs for sources 1 and 2, as well as Charlie's ancilla state. In our visualization, mutually coherent pulse pairs are prepared using an asymmetric interferometer placed after the master laser. The pump beam is then equally split into three pulse pairs to pump the three PEPSs. Each PEPS can be readily constructed, for example, using three-wave mixing in a nonlinear medium [61].

We consider the ancillary state $|\psi_A\rangle_{m,n} = \frac{1}{2}(|1,2\rangle_{m,n} + |2,1\rangle_{m,n} + |3,4\rangle_{m,n} + |4,3\rangle_{m,n})$, which is just a symmetric four-dimensional form of the state (4), and does not change the derivation presented in Sec. II. This ancillary state is equivalent to the hyper-entangled state

$$|\psi_A\rangle_{m,n} = \frac{1}{2}(|H(t_e), V(t_e)\rangle_{m,n} + |V(t_e), H(t_e)\rangle_{m,n} + |H(t_l), V(t_l)\rangle_{m,n} + |V(t_l), H(t_l)\rangle_{m,n}).$$

Preparing the ancilla state becomes significantly easier in a hyper-entangled system. This is because any polarization-entangled two-photon qubit state can be transformed into any desired pure state within the two-qubit polarization subspace using only linear optical elements.

The BSA setup is identical to Fig. 1 for hyper-entanglement, with the addition of a polarizer in each of the four arms. These polarizers have a fixed projection angle, enabling post-selection alongside temporal mode selection. The final swapped state between Alice and Bob can be characterized using entangled state analyzers (ESA). Each ESA consists of a postselection-free Franson interferometer [62, 63].

IV. CONCLUSION

In this work, we have presented a scheme for implementing HD entanglement swapping using only linear optical elements and ancillary photons. Previous work [48] proposed a related approach based on the QFT for HD Bell state analysis, tailored to time-bin encoding

in even-dimensional systems. The presented scheme requires fewer beam splitter operations, which can be a decisive advantage when the HOM visibility is limited. Here, we considered only entanglement swapping of dimensions up to six, which must be experimentally feasible to realize. Nevertheless, an efficient optical design, combined with PNR detection, is essential for achieving both a high success probability and acceptable fidelity. Interestingly, the proposed scheme yields two-dimensional entanglement swapping for certain detection events and surpasses the conventional 50% limit of setups based solely on passive, linear optical elements. Finally, we proposed a simple experimental approach for realizing four-dimensional hyper-entanglement swapping using time-bin and polarization DOFs.

We acknowledge the support from Carl-Zeiss-Stiftung (CZS) via the CZS Center for Quantum Photonics QPhoton.

Appendix A: Three-dimensional entanglement swapping

While the ancilla state remains unchanged, the initial three-dimensional states must have the form

$$|\psi_I\rangle_{m,n} = \frac{1}{\sqrt{3}}(|1,2\rangle_{m,n} + |2,1\rangle_{m,n} + |3,4\rangle_{m,n}), \quad (\text{A1})$$

or

$$|\psi_I\rangle_{m,n} = \frac{1}{\sqrt{3}}(|1,1\rangle_{m,n} + |2,2\rangle_{m,n} + |3,4\rangle_{m,n}), \quad (\text{A2})$$

where the relative phase between modes can be chosen arbitrarily. These states are three-dimensional maximally entangled, but embedded in a four-dimensional space. In the three-dimensional scenario, the total number of possible mode combinations is 772 for the state (A1), of which 68 combinations correspond to six-photon detection events. Among these, only four lead to the projection of photons in modes a and d into the normalized three-dimensional maximally entangled state:

$$|\psi\rangle_{a,d} = \frac{1}{\sqrt{3}}(|1,2\rangle_{a,d} - |2,1\rangle_{a,d} + |3,4\rangle_{a,d}). \quad (\text{A3})$$

Even though the initial states are defined in a four-dimensional subspace, the conditional efficiency for the three-dimensional entanglement swapping is higher than that for the four-dimensional scenario.

[1] H.-J. Briegel, W. Dür, J. I. Cirac, and P. Zoller, *Phys. Rev. Lett.* **81**, 5932 (1998).
[2] L.-M. Duan, M. D. Lukin, J. I. Cirac, and P. Zoller, *Nature* **414**, 413 (2001).
[3] Z. Zhao, T. Yang, Y.-A. Chen, A.-N. Zhang, and J.-W. Pan, *Phys. Rev. Lett.* **90**, 207901 (2003).
[4] A. M. Goebel, C. Wagenknecht, Q. Zhang, Y.-A. Chen, K. Chen, J. Schmiedmayer, and J.-W. Pan, *Phys. Rev. Lett.* **101**, 080403 (2008).

[5] S.-K. Liao, W.-Q. Cai, W.-Y. Liu, L. Zhang, Y. Li, J.-G. Ren, J. Yin, Q. Shen, Y. Cao, Z.-P. Li, F.-Z. Li, X.-W. Chen, L.-H. Sun, J.-J. Jia, J.-C. Wu, X.-J. Jiang, J.-F. Wang, Y.-M. Huang, Q. Wang, Y.-L. Zhou, L. Deng, T. Xi, L. Ma, T. Hu, Q. Zhang, Y.-A. Chen, N.-L. Liu, X.-B. Wang, Z.-C. Zhu, C.-Y. Lu, R. Shu, C.-Z. Peng, J.-Y. Wang, and J.-W. Pan, *Nature* **549**, 43 (2017).

[6] J. Yin, Y. Cao, Y.-H. Li, S.-K. Liao, L. Zhang, J.-G. Ren, W.-Q. Cai, W.-Y. Liu, B. Li, H. Dai, G.-B. Li, Q.-M. Lu, Y.-H. Gong, Y. Xu, S.-L. Li, F.-Z. Li, Y.-Y. Yin, Z.-Q. Jiang, M. Li, J.-J. Jia, G. Ren, D. He, Y.-L. Zhou, X.-X. Zhang, N. Wang, X. Chang, Z.-C. Zhu, N.-L. Liu, Y.-A. Chen, C.-Y. Lu, R. Shu, C.-Z. Peng, J.-Y. Wang, and J.-W. Pan, *Science* **356**, 1140 (2017), <https://www.science.org/doi/pdf/10.1126/science.aan3211>.

[7] C. H. Bennett, G. Brassard, C. Crépeau, R. Jozsa, A. Peres, and W. K. Wootters, *Phys. Rev. Lett.* **70**, 1895 (1993).

[8] M. Żukowski, A. Zeilinger, M. A. Horne, and A. K. Ekert, *Phys. Rev. Lett.* **71**, 4287 (1993).

[9] D. Bouwmeester, J.-W. Pan, K. Mattle, M. Eibl, H. Weinfurter, and A. Zeilinger, *Nature* **390**, 575 (1997).

[10] J.-W. Pan, D. Bouwmeester, H. Weinfurter, and A. Zeilinger, *Phys. Rev. Lett.* **80**, 3891 (1998).

[11] S. Ghosh, G. Kar, A. Roy, D. Sarkar, and U. Sen, *New Journal of Physics* **4**, 48 (2002).

[12] R.-B. Jin, M. Takeoka, U. Takagi, R. Shimizu, and M. Sasaki, *Scientific Reports* **5**, 9333 (2015).

[13] S. Hassanpour and M. Houshmand, *Quantum Information Processing* **15**, 905 (2016).

[14] X.-M. Hu, Y. Guo, B.-H. Liu, C.-F. Li, and G.-C. Guo, *Nature Reviews Physics* **5**, 339 (2023).

[15] M. J. Bayerbach, S. E. D'Aurelio, P. van Loock, and S. Barz, *Science Advances* **9**, eadf4080 (2023), <https://www.science.org/doi/pdf/10.1126/sciadv.adf4080>.

[16] B. Alipour and A. Akhound, *International Journal of Theoretical Physics* **63**, 140 (2024).

[17] S. E. D'Aurelio, M. J. Bayerbach, and S. Barz, *npj Quantum Information* **11**, 37 (2025).

[18] S. Bose, V. Vedral, and P. L. Knight, *Phys. Rev. A* **57**, 822 (1998).

[19] C.-Y. Lu, T. Yang, and J.-W. Pan, *Phys. Rev. Lett.* **103**, 020501 (2009).

[20] X. Su, C. Tian, X. Deng, Q. Li, C. Xie, and K. Peng, *Phys. Rev. Lett.* **117**, 240503 (2016).

[21] M. Erhard, R. Fickler, M. Krenn, and A. Zeilinger, *Light: Science & Applications* **7**, 17146 (2018).

[22] D. Cozzolino, B. Da Lio, D. Bacco, and L. K. Oxenløwe, *Advanced Quantum Technologies* **2**, 1900038 (2019), <https://advanced.onlinelibrary.wiley.com/doi/pdf/10.1002/qute.201900038>.

[23] Z.-X. Cui, W. Zhong, L. Zhou, and Y.-B. Sheng, *Science China Physics, Mechanics & Astronomy* **62**, 110311 (2019).

[24] H.-S. Zhong, H. Wang, Y.-H. Deng, M.-C. Chen, L.-C. Peng, Y.-H. Luo, J. Qin, D. Wu, X. Ding, Y. Hu, P. Hu, X.-Y. Yang, W.-J. Zhang, H. Li, Y. Li, X. Jiang, L. Gan, G. Yang, L. You, Z. Wang, L. Li, N.-L. Liu, C.-Y. Lu, and J.-W. Pan, *Science* **370**, 1460 (2020), <https://www.science.org/doi/pdf/10.1126/science.abe8770>.

[25] L. S. Madsen, F. Laudenbach, M. F. Askarani, F. Rortais, T. Vincent, J. F. F. Bulmer, F. M. Miatto, L. Neuhaus, L. G. Helt, M. J. Collins, A. E. Lita, T. Gerrits, S. W. Nam, V. D. Vaidya, M. Menotti, I. Dhand, Z. Vernon, N. Quesada, and J. Lavoie, *Nature* **606**, 75 (2022).

[26] S. Wehner, D. Elkouss, and R. Hanson, *Science* **362**, eaam9288 (2018), <https://www.science.org/doi/pdf/10.1126/science.aam9288>.

[27] J. Bouda and V. Buzek, *Journal of Physics A: Mathematical and General* **34**, 4301 (2001).

[28] P. Zhou, F.-G. Deng, and H.-Y. Zhou, *Physica Scripta* **79**, 035005 (2009).

[29] E. V. Kovlakov, S. S. Straupe, and S. P. Kulik, *Phys. Rev. A* **98**, 060301 (2018).

[30] S. Liu, Z. Zhou, S. Liu, Y. Li, Y. Li, C. Yang, Z. Xu, Z. Liu, G. Guo, and B. Shi, *Phys. Rev. A* **98**, 062316 (2018).

[31] B. Baghdasaryan, C. Sevilla-Gutiérrez, F. Steinlechner, and S. Fritzsche, *Phys. Rev. A* **106**, 063711 (2022).

[32] R. Bernecker, B. Baghdasaryan, and S. Fritzsche, *Phys. Rev. A* **110**, 033718 (2024).

[33] H. Zhang, C. Zhang, X.-M. Hu, B.-H. Liu, Y.-F. Huang, C.-F. Li, and G.-C. Guo, *Phys. Rev. A* **99**, 052301 (2019).

[34] Y.-B. Sheng, F.-G. Deng, and G. L. Long, *Phys. Rev. A* **82**, 032318 (2010).

[35] Q. Zhang, A. Goebel, C. Wagenknecht, Y.-A. Chen, B. Zhao, T. Yang, A. Mair, J. Schmiedmayer, and J.-W. Pan, *Nature Physics* **2**, 678 (2006).

[36] X.-L. Wang, X.-D. Cai, Z.-E. Su, M.-C. Chen, D. Wu, L. Li, N.-L. Liu, C.-Y. Lu, and J.-W. Pan, *Nature* **518**, 516 (2015).

[37] Y. Zhang, M. Agnew, T. Roger, F. S. Roux, T. Konrad, D. Faccio, J. Leach, and A. Forbes, *Nature Communications* **8**, 632 (2017).

[38] S. Merkouche, V. Thiel, A. O. C. Davis, and B. J. Smith, *Phys. Rev. Lett.* **128**, 063602 (2022).

[39] X.-M. Hu, C. Zhang, B.-H. Liu, Y. Cai, X.-J. Ye, Y. Guo, W.-B. Xing, C.-X. Huang, Y.-F. Huang, C.-F. Li, and G.-C. Guo, *Phys. Rev. Lett.* **125**, 230501 (2020).

[40] Y.-H. Luo, H.-S. Zhong, M. Erhard, X.-L. Wang, L.-C. Peng, M. Krenn, X. Jiang, L. Li, N.-L. Liu, C.-Y. Lu, A. Zeilinger, and J.-W. Pan, *Phys. Rev. Lett.* **123**, 070505 (2019).

[41] Z. Zeng, *Opt. Lett.* **47**, 5817 (2022).

[42] M.-Y. Lv, X.-M. Hu, N.-F. Gong, T.-J. Wang, Y. Guo, B.-H. Liu, Y.-F. Huang, C.-F. Li, and G.-C. Guo, *Science China Physics, Mechanics & Astronomy* **67**, 230311 (2024).

[43] L. Bianchi, C. Marconi, J. Sperling, and D. Bacco, *Phys. Rev. Res.* **7**, 023038 (2025).

[44] X. Qiu, H. Guo, and L. Chen, “Quantum teleportation of high-dimensional spatial modes: Towards an image teleportation,” *arXiv:2112.03764 [physics.optics]*.

[45] B. Sephton, A. Vallés, I. Nape, M. A. Cox, F. Steinlechner, T. Konrad, J. P. Torres, F. S. Roux, and A. Forbes, *Nature Communications* **14**, 8243 (2023).

[46] H. Zhang, L. Wan, T. Haug, W.-K. Mok, S. Paezani, Y. Shi, H. Cai, L. K. Chin, M. F. Karim, L. Xiao, X. Luo, F. Gao, B. Dong, S. Asaad, M. S. Kim, A. Laing, L. C. Kwek, and A. Q. Liu, *Science Advances* **8**, eabn9783 (2022), <https://www.science.org/doi/pdf/10.1126/sciadv.abn9783>.

[47] C. Zhang, J. F. Chen, C. Cui, J. P. Dowling, Z. Y. Ou, and T. Byrnes, *Phys. Rev. A* **100**, 032330 (2019).

[48] N. Bharos, L. Markovich, and J. Borregaard, *Quantum* **9**, 1711 (2025).

[49] W. R. Clements, P. C. Humphreys, B. J. Metcalf, W. S. Kolthammer, and I. A. Walmsley, *Optica* **3**, 1460 (2016).

[50] M. Halder, A. Beveratos, N. Gisin, V. Scarani, C. Simon, and H. Zbinden, *Nature Physics* **3**, 692 (2007).

[51] Q.-C. Sun, Y.-L. Mao, Y.-F. Jiang, Q. Zhao, S.-J. Chen, W. Zhang, W.-J. Zhang, X. Jiang, T.-Y. Chen, L.-X. You, L. Li, Y.-D. Huang, X.-F. Chen, Z. Wang, X. Ma, Q. Zhang, and J.-W. Pan, *Phys. Rev. A* **95**, 032306 (2017).

[52] Q.-C. Sun, Y.-F. Jiang, Y.-L. Mao, L.-X. You, W. Zhang, W.-J. Zhang, X. Jiang, T.-Y. Chen, H. Li, Y.-D. Huang, X.-F. Chen, Z. Wang, J. Fan, Q. Zhang, and J.-W. Pan, *Optica* **4**, 1214 (2017).

[53] F. Samara, N. Maring, A. Martin, A. S. Raja, T. J. Kippenberg, H. Zbinden, and R. Thew, *Quantum Science and Technology* **6**, 045024 (2021).

[54] T. S. Humble and W. P. Grice, *Phys. Rev. A* **77**, 022312 (2008).

[55] Y. Tsujimoto, M. Tanaka, N. Iwasaki, R. Ikuta, S. Miki, T. Yamashita, H. Terai, T. Yamamoto, M. Koashi, and N. Imoto, *Scientific Reports* **8**, 1446 (2018).

[56] M. Zopf, R. Keil, Y. Chen, J. Yang, D. Chen, F. Ding, and O. G. Schmidt, *Phys. Rev. Lett.* **123**, 160502 (2019).

[57] F. Wang, M. Erhard, A. Babazadeh, M. Malik, M. Krenn, and A. Zeilinger, *Optica* **4**, 1462 (2017).

[58] J. Calsamiglia, *Phys. Rev. A* **65**, 030301 (2002).

[59] F. Ewert and P. van Loock, *Phys. Rev. Lett.* **113**, 140403 (2014).

[60] T. Yamazaki and K. Azuma, *Phys. Rev. Lett.* **134**, 200801 (2025).

[61] A. Anwar, C. Perumangatt, F. Steinlechner, T. Jennewein, and A. Ling, *Review of Scientific Instruments* **92**, 041101 (2021), https://pubs.aip.org/aip/rsi/article-pdf/doi/10.1063/5.0023103/19759999/041101_1_online.pdf.

[62] D. Strekalov, T. Pittman, A. Sergienko, Y. Shih, and P. Kwiat, *Physical Review A* **54**, R1 (1996).

[63] L. Bulla, M. Pivoluska, K. Hjorth, O. Kohout, J. Lang, S. Ecker, S. P. Neumann, J. Bittermann, R. Kindler, M. Huber, et al., *Physical Review X* **13**, 021001 (2023).